Changes by Butterflies: Farsighted Forecasting with Group Reservoir Transformer

Md Kowsher and Abdul Rafae Khan and Jia Xu

Abstract

In Chaos, a minor divergence between two initial conditions exhibits exponential amplification over time, leading to far-away outcomes, known as the butterfly effect. Thus, the distant future is full of uncertainty and hard to forecast. We introduce Group Reservoir Transformer to predict long-term events more accurately and robustly by overcoming two challenges in Chaos: (1) the extensive historical sequences and (2) the sensitivity to initial conditions. A reservoir is attached to a Transformer to efficiently handle arbitrarily long historical lengths, with an extension of a group of reservoirs to reduce the sensitivity to the initialization variations. Our architecture consistently outperforms state-of-the-art models in multivariate time series, including TimeLLM, GPT2TS, PatchTST, DLinear, TimeNet, and the baseline Transformer, with an error reduction of up to -59% in various fields such as ETTh, ETTm, and air quality, demonstrating that an ensemble of butterfly learning can improve the adequacy and certainty of event prediction, despite of the traveling time to the unknown future.

1 Introduction

Chaos theory offers a framework that underlies patterns and deterministic laws governing dynamical systems, applied in human society, such as biology, chemistry, physics, economics, and mathematics, among others [Liu, 2010]. Chaos are hard to predict due to the "butterfly effect" [Jordan and Smith, 2007], i.e., when two initial conditions exhibit only a minor disparity, their divergence over time undergoes exponential amplification, contingent upon the Lyapunov time inherent to the system's dynamics [Wu et al., 2024]. Consequently, forecasting the distant future in chaotic systems presents formidable challenges primarily rooted in two fundamental issues: (1) the need to account for extensive historical sequences and (2) the pronounced sensitivity to initial conditions.

Prior research has explored a multitude of techniques in chaotic event prediction, with a notable emphasis on the utilization of deep neural network models, exemplified by Transformer [Zeng et al., 2022]. Nevertheless, the Transformer architecture's quadratic time and memory complexity of the input length significantly limits the performance of long-term forecasting tasks [Vaswani et al., 2017]. Several notable efforts, including but not limited to UnlimiFormer [Bertsch et al., 2023], Efficient Transformer [Tay et al., 2022], and Reformer [Kitaev et al., 2020], extend the input length of Transformers but primarily hinge on modifications to the attention model itself, often founded on certain assumptions to extend the input length to a fixed value without considering the temporal dependency of the very far away events, thereby yielding limited adaptability for learning from and predicting arbitrary long sequences.

Stream reservoir learning: We integrate reservoir computing, as an autoregressive model, into the Transformer framework that effectively models sequences of inputs with arbitrary lengths. Reservoir computing, known for its simplicity and computational efficiency, excels in processing temporal data within the context of chaotic time series prediction [Bollt, 2021]. Within our architecture, the reservoir captures dependencies across all temporal events by discerning the sequence of events based on all historical data without window-sized context restriction. The reservoir learning processes the

input in a stream fashion and requires **no training** by freezing reservoir weights. Its linear time complexity and the constant space complexity to the input length make handling the arbitrary context length possible. Subsequently, the Transformer digests short-term events in quadratic time, melding its insights with long-term events modeled by the reservoir to produce a more accurate final forecast. Our framework grapples with two technical obstacles related to Lyapunov time and the butterfly effect using the following two techniques: nonlinear readout and group reservoir.

Non-linearity: The traditional linear readout is expensive since the number of reservoir nodes scales quadratically with the reservoir output size, which mirrors the input size of the Transformer. Our system employs a nonlinear readout rooted in single-head attention mechanisms to manage longer sequences efficiently, superseding the traditional linear reservoir readout. Given its heightened expressiveness, this nonlinear readout reduces reservoir outputs' dimensionality, thus providing the Transformer with more meaningful and potent feature inputs and dimension reduction.

Group reservoir: To stabilize the sensitivities on varied initializations, we incorporate ensemble learning using multiple reservoirs, we term "group reservoirs". Each reservoir in the group takes a random initialization, and the output from their ensemble seamlessly integrates with the observation of the recent events modeled by the Transformer, facilitating short-term context comprehension.

Empirical results demonstrate that the nonlinear readout and group reservoir drastically improve the Transformer and its variants in time-series predictions with an error reduction of up to 59.70%. Our methodology surpasses Transformer and other leading-edge deep neural networks (DNNs). It aptly handles very long input lengths, signaling a notable improvement for the Transformer model.

Our contributions are mainly fourfold: (1) We integrate reservoir computing into the system, enabling the Transformer to tackle long-term predictions effectively. (2) We refine traditional reservoir computing techniques by improving the linear readout with a nonlinear counterpart, facilitating streamlined dimensionality reduction while keep the autoregressive learning on temporal patterns. (3) We implement the group reservoir to address the nuances of reservoir initialization sensitivity. (4) Our approach demonstrated superior performance in forecasting chaotic phenomena in long-term horizons. Furthermore, it achieved state-of-the-art results in forecasting multivariate time series data.

2 Background

Preliminary: We consider a time series dataset denoted by $\mathbf{u}_{1:T}$, where each element $\mathbf{u}_t \in \mathbb{R}^{N_u}$ represents a N_u -dimensional vector at time $t \in \{1, \cdots, T\}$. Given a rolling forecasting scenario with a fixed window size w, our objective is to predict τ future time steps, $\mathbf{u}_{t+1:t+\tau}$, based on the input $\mathbf{u}_{t-w:t}$. We propose the following model:

$$\hat{\mathbf{u}}_{t+1:t+\tau} = \mathbb{M}(\mathbf{u}_{t-w:t}, \mathbf{\Phi}) \tag{1}$$

Here, Φ represents learnable parameters, and $\mathbb{M}(\cdot)$ is a Transformer time-series forecasting model.

3 Method

Transformer has a quadratic time complexity in terms of the history length and prediction future time steps [Jin et al., 2024, Nie et al., 2022, Beltagy et al., 2020]. To reduce the computational complexity of window sizes, we introduce reservoir computing $\mathcal R$ to model the entire history of the time series efficiently:

$$\hat{\mathbf{u}}_{t+1:t+\tau} = \mathbb{M}(\mathbf{u}_{t-k:t} \uplus \mathcal{R}(\mathbf{u}_{1:T}), \mathbf{\Phi})$$
(2)

Here, \mathcal{R} is a Reservoir, which takes input as time steps sequentially and outputs m size vectors. The concatenation operator \forall combines the short-term window $\mathbf{u}_{t-k:t}$ with the long-term historical context $\mathcal{R}(\mathbf{u}_{1:T})$. The resulting effective input size is significantly smaller, $m+k \ll w$, where k is the reduced window size, and \mathcal{R} handles all history without input length restriction. Below, we will describe how to model \mathcal{R} is a Reservoir.

3.1 Cross-attention for Embedding

We first embed the time series data for the neural networks. Since the embedding window has a fixed size, time series sequential input usually are chunked into segments, and the learning happens segment

by segment. To make each segment comparable to the others, the full time series input are often normalized. Here we use the reversible instance normalization technique for normalization [Kim et al., 2021, Zhou et al., 2021, Wu et al., 2021, Liu et al., 2021], where the full sequence $\mathbf{u}_{1:T}$ is normalized to have zero mean and unit variance. We denote each token embedding as $\epsilon(\mathbf{u_t}) \in \mathbb{R}^{d_\epsilon}$, where $\mathbf{u}_t \in \mathbb{R}^{d_u}$, and the input $\mathbf{u}_{1:T}$ is embedded into $\epsilon(\mathbf{u}_1), \epsilon(\mathbf{u}_2), \ldots, \epsilon(\mathbf{u}_T)$. To address the dependency of each time step in one segment, we apply the cross-attention [Zhang and Yan, 2022, Rombach et al., 2022], where each vector $\epsilon(\mathbf{u}_{t-k:t})$ considers the local temporal relationship with its i-window-sized neighbors $\epsilon(\mathbf{u}_{t-i:t+i})$:

$$\mathbf{h}_{t} = \operatorname{softmax}\left(\frac{\mathbf{W}_{k} \cdot \epsilon(\mathbf{u}_{t-k:t})(\mathbf{W}_{q} \cdot \epsilon(\mathbf{u}_{t-i:t+i}))^{T}}{\sqrt{d_{\epsilon}}}\right) \mathbf{W}_{v} \cdot \epsilon(\mathbf{u}_{t-i:t+i}), \tag{3}$$

where $\mathbf{h}_t \in \mathbb{R}^{k \times d_{\epsilon}}$ carries the local temporal relationship for time step t. Here \mathbf{W}_q , \mathbf{W}_k , \mathbf{W}_v are trainable matrices to learn queries, keys, and values, respectively [Wei et al., 2020].

3.2 Deep Reservoir Computing

The Echo State Network (ESN) [Jaeger and Haas, 2004] implements discrete-time dynamical systems as one of the reservoir computing frameworks [Lukoševičius and Jaeger, 2009, Verstraeten et al., 2007]. The recurrent reservoir layers are untrained and provide a suffix-based Markovian representation of the past input history [Tiňo et al., 2007], attaching a trained linear readout.

We use the Leaky Integrator ESN (LI-ESN) model [Jaeger et al., 2007], a variant of the basic ESN, in which leaky integrator reservoir units are adopted. In a LI-ESN with N_u input units and N_r reservoir units the state is updated according to the following state transition function:

$$\mathbf{x}_{t} = (1 - \alpha)\mathbf{x}_{t-1} + \alpha \tanh(\mathbf{W}_{in}\mathbf{h}_{t} + \boldsymbol{\theta} + \mathbf{W}\mathbf{x}_{t-1}), \tag{4}$$

where $\mathbf{x}_t \in \mathbb{R}^{N_r}$ denote the input and the reservoir state at time t, respectively. $\mathbf{W}_{in} \in \mathbb{R}^{N_r \times d_\epsilon}$ is the input-to-reservoir weight matrix, $\boldsymbol{\theta} \in \mathbb{R}^{N_r}$ is the bias-to-reservoir weight vector. $\mathbf{W} \in \mathbb{R}^{N_r \times N_r}$ is the recurrent reservoir weight matrix, t anh is the element-wise hyperbolic tangent activation function, and $\alpha \in [0,1]$ is the leaky parameter. The reservoir parameters are initialized according to the constraints specified by the Echo State Property (ESP) [Jaeger and Haas, 2004, Tiňo et al., 2007] and then are left untrained, which makes its computing efficient. Accordingly, the weight values in \mathbf{W}_{in} and in $\boldsymbol{\theta}$ are chosen from a uniform distribution over $[-\sigma_{in}, \sigma_{in}]$, where σ_{in} represents an input-scaling parameter. The values in matrix \mathbf{W} are randomly selected from a uniform distribution and then re-scaled such that the spectral radius (i.e. the largest eigenvalue in absolute value) of matrix $\mathbf{W} = (1-\alpha)I + \alpha \mathbf{W}$, denoted by ρ , is smaller than 1, i.e. $\rho < 1$ [Jaeger and Haas, 2004]. Note that the leaky parameter α and the spectral radius of the recurrent weight matrix ρ represent two relevant reservoir computing hyper-parameters. α is set to a fixed value of 0.7 for simplicity, and ρ is uniform randomly sampled between [0,1].

3.3 Linear Readout

As reservoir output, a readout component is used to linearly combine the outputs of all the reservoir units as in a standard ESN. The output of a reservoir at each time step t can be computed as

$$\mathbf{y}_t = \mathbf{W}_{out} \mathbf{x}_t + \boldsymbol{\theta}_{out}, \tag{5}$$

where $\mathbf{y}_t \in \mathbb{R}^m$ is the linear readout with m dimensionality. $\mathbf{W}_{out} \in \mathbb{R}^{m \times N_r}$ represents the reservoir-to-readout weight matrix, connecting the reservoir units to the units in the readout. $\boldsymbol{\theta}_{out} \in \mathbb{R}^m$ is the bias-to-readout weight vector. Training the readout involves solving a linear regression problem, typically approached by using Moore-Penrose pseudo-inversion, with further details in Lukoševičius and Jaeger [2009], Jaeger and Haas [2004]. Since only \mathbf{W}_{out} are trained, the optimization problem boils down to linear regression.

3.4 Nonlinear Readout

The output of the reservoir is the input of the Transformer. One downside of the reservoir is that if the reservoir output size is large, then the Transformer training will be slow due to its quadratic

complexity to its input size. Since a linear readout of a reservoir needs a much larger size to have the same expressive power as the nonlinear readout, we introduce nonlinear readout layers, which work quite well in reducing reservoir output dimension and improving prediction performance hereafter. Therefore, for a faster convergence and avoiding a local optimum [Triefenbach and Martens, 2011], we append a nonlinear readout to the linear readout using the following non-linear activation function:

$$\mathbf{\Lambda}_t^l = \sigma(\mathbf{y}_t^l),\tag{6}$$

where $\sigma(\mathbf{y}_t^l)$ is the l-th reservoir output, and we use L many reserviors in the following section.

3.5 Group Reservoir

In Chaos theory, the butterfly effect refers to the sensitive dependence on initial conditions, where a small change in one state of a deterministic nonlinear system can result in large differences in a later state. As ensemble reduces the variants of the prediction, we integrate multiple reservoirs' nonlinear readout layers for the stability of our prediction. We consider L reservoirs, each with distinct decay rates (α and ρ), initialized randomly [Gallicchio et al., 2017]. This results in a grouped Echo State Network (ESN) representation o_t , achieved by element-wise \oplus addition of all reservoirs' non-linear activation outputs:

$$\mathbf{o}_t = \mathbf{\Lambda}_t^1 \oplus \mathbf{\Lambda}_t^2 \oplus \ldots \oplus \mathbf{\Lambda}_t^L \tag{7}$$

Group Reservoir Readout with Self-Attention 3.6

In order to capture the input feature importance, alleviating the problem of vanishing gradient of long-distance dependency, we have used a self-attention mechanism from the aggregate output of group reservoir in Equation 7 by following Shaw et al. [2018]:

$$e_{ij} = \frac{(\mathbf{o}_t^i W^Q)(\mathbf{o}_t^j W^K)^T}{\sqrt{d_{\epsilon}}}$$

$$\alpha_{ij} = \frac{\exp e_{ij}}{\sum_{k=1}^n \exp e_{ik}}$$
(8)

$$\alpha_{ij} = \frac{\exp e_{ij}}{\sum_{k=1}^{n} \exp e_{ik}} \tag{9}$$

$$\mathbf{z_t} = \sum_{i=1}^{n} \alpha_{ij} (\mathbf{o}_t^j W^V) \tag{10}$$

Group Reservoir Transformer (RT) 3.7

Our group reservoir efficiently models observed time-series data in dynamical systems and require minimal training data and computing resources [Gauthier et al., 2021] and is ideal for handling long sequential inputs. Here we mainly describe adopting a reservoir for Transformer as one of the most well-known DNN architectures. However, our methods are adaptable to other DNN model architectures, for whom we also compared results in our experiments.

Figure 1 (Left) shows the architecture of our reservoir-enhanced Transformer. We enhance the nonlinear readout layers through self-attention mechanisms within ensemble reservoirs. This involves updating these layers and performing element-wise addition of the readouts, resulting in an output denoted as \mathbf{z}_t . This output is concatenated with the present input embedding \mathbf{h}_t , yielding \mathbf{f}_t , which then undergoes processing via the Transformer encoder $\mathbb{M}(.)$.

Our approach enables comprehensive modeling of entire historical data in decision-making. While the Transformer captures temporal dependencies, limited by a window of size w, our method incorporates reservoir pooling to overcome this limitation. This permits the consideration of the entire history without a rise in time complexity. By incorporating Equation 7 (ensemble of all L reservoir readouts) and then following Equation 10, we have:

$$\mathbf{f}_t = (1 - \kappa)\mathbf{z}_t \uplus \kappa \mathbf{h}_t \tag{11}$$

$$\hat{\mathbf{u}}_{t+1:t+\tau} = \mathbb{M}(\mathbf{f}_t) \tag{12}$$

Here, \uplus is the concatenation between group reservoirs readout and input time sequence, $\mathbf{f}_t \in \mathbb{R}^{m+k}$ denotes the input of Transformer M and κ is a learnable parameter indicating the weights of input

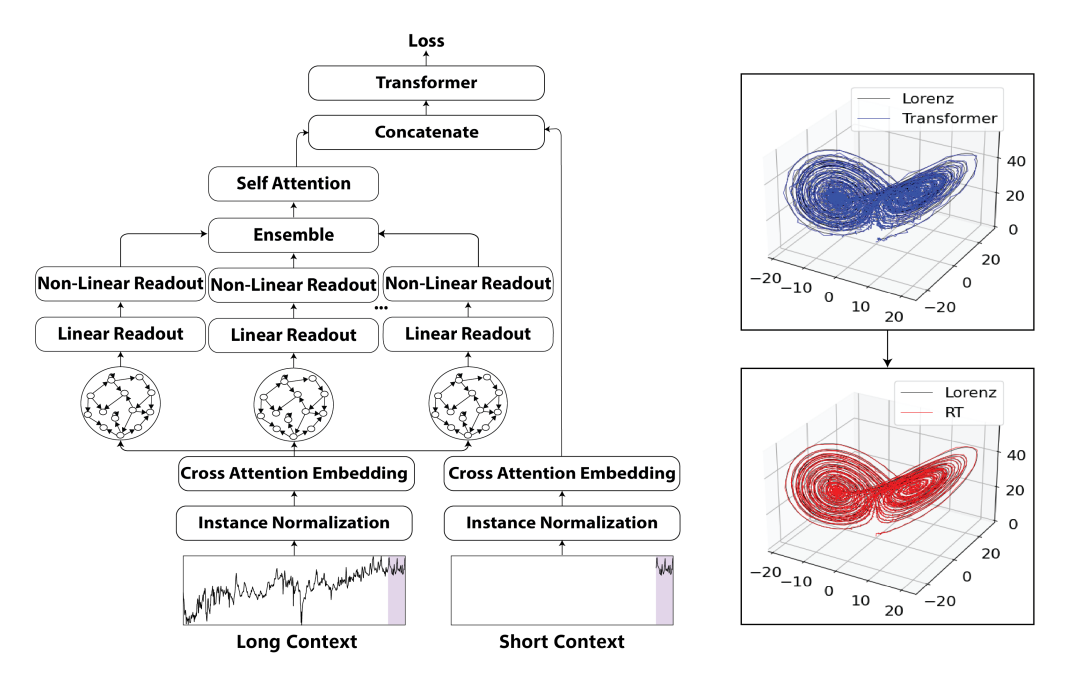


Figure 1: Left: Group Reservoir Transformer; Right: Our RT prediction is closer to the ground truth than the Transformer in Lorenz Extractor.

states and reservoir readout to predict $\hat{\mathbf{u}}_{t+1:t+\tau}$ by Equation 12 as a realization of Equation 2. \mathbf{z}_t is trained on the full historical sequence, and \mathbf{h}_t is trained only on the most recent short history.

3.8 Training

In this work, we use the Huber loss function [Meyer, 2021] as our objective (Equation 13):

$$\mathcal{L}(\mathbf{u}_{t+1:t+\tau}, \hat{\mathbf{u}}_{t+1:t+\tau}) = \frac{1}{\tau} \sum_{i=t+1}^{t+\tau} \begin{cases} \frac{1}{2} (\mathbf{u}_i - \hat{\mathbf{u}}_i)^2, & \text{if } |\mathbf{u}_i - \hat{\mathbf{u}}_i| \le \delta \\ \delta(|\mathbf{u}_i - \hat{\mathbf{u}}_i| - \frac{1}{2}\delta), & \text{otherwise} \end{cases}$$
(13)

Here δ is an adjustable parameter that controls where the function change occurs to keep the function differentiable. For a comprehensive understanding of our training algorithm, refer to the pseudo-code provided in the Appendix B, along with a detailed explanation of the notation employed. Initially, we sequentially train the model $\mathbb{M}(.)$ across all T time stamps using all the training dataset. Subsequently, we fine-tune our model using the validation set to achieve optimal model performance. The model is subjected to testing with varying hyper-parameters such as reservoir size, leaky rate, spectral radius, number of reservoirs, learning rate, attention size, Transformer block, and dropout rate. The choice of these hyper-parameters may differ depending on the specific dataset with details in Appendix A.

4 Experiments

Baselines: We use well-known time-series forecasting models for our baseline comparisons, including Transformer based systems such as DLinear [Zeng et al., 2023], PatchTST [Nie et al., 2022], TimesNet [Wu et al., 2022a], FEDformer [Zhou et al., 2022], Stationary [Liu et al., 2022], ESTformer [Woo et al., 2022], LightTS [Campos et al., 2023], and Autoformer [Chen et al., 2021], and pre-trained LLMs-based systems such as TimeLLM [Jin et al., 2024] and GPT2TS [Zhou et al., 2024]. The experimental setup follows [Zeng et al., 2023] for all baseline models.

Datasets: We evaluate RT on several datasets commonly used for benchmarking long-term multivariate forecasting models, including four ETT datasets (ETTh1, ETTh2, ETTm1, and ETTm2) [Zhou et al., 2021], Weather, Electricity (ECL), Traffic, and ILI from Zeng et al. [2022]. To test the chaotic behavior on these datasets, we employ the correlation dimension, denoted as D_2 to serve as a reliable measure of chaotic behavior, with higher values reflecting more pronounced chaos [Pánis et al., 2020].

We compute correlation dimension D_2 across multiple datasets using diverse state numbers (100, 500, and 1000). Table 1 shows the D_2 of each dataset.

Length	ETTh1	ETTh2	ETTm1	ETTm2	DDFO	Exchange	ILI	BTC	DGP	DWV	MGS	ECG	LA
100	0.790	1.190	0.560	0.299	0.540	0.995	0.995	0.961	1.070	1.343	3.242	2.913	2.515
500	1.340	0.973	0.931	0.535	0.540	1.099	1.249	0.853	1.626	1.823	3.452	3.173	2.721
1000	1.266	0.866	1.061	0.667	0.540	1.359	1.299	0.853	1.398	1.838	3.531	3.282	2.841
			low chao			medi	ium cha	0		ŀ	igh cha	О	

Table 1: D_2 chaotic behavior measure: MGS, ECG, LA are high chaos; ETTh are low chaos.

Results: The time-series forecasting prediction error rate results are presented in Table 2. The input time series length k is set to 300, and we test four different prediction horizons $h \in \{96, 192, 336, 720\}$. The evaluation metrics are mean square error (MSE) and mean absolute error (MAE). Our RT consistently outperforms all baselines in most cases, achieving significant error reductions. Specifically, compared to DLinear, RT reduces MSE by an average of 4.2%. Similarly, the reductions in MSE for PatchTST and TimeNet are 1.4% and 2.4%, respectively. Additionally, RT outperforms pre-trained LLM-based time series models in Table 3. Table 4 shows that RT model outperforms baseline Transformer on various datasets: Air Quality (AQ), Daily Website Visitors (DWV), Daily Gold Price (DGP), Daily Demand Forecasting Orders (DDF), Bitcoin Historical Dataset (BTC), Absenteeism at Work (AW), and Temperature Readings (TR). All results are reported in MSE and MAE values, with only AW and TR reporting Accuracy and F-Score metrics. Comparisons with more baselines in other evaluation criteria are detailed in Appendix F.

Method	ls		RT urs)		near (23)		hTST 023)		esNet (23)	FEDf (20	ormer		onary (22)		ormer
Metric	;	MSE	MAE	MSE	MAE	MSE	MAE	MSE	MAE	MSE	MAE	MSE	MAE	MSE	MAE
	96	0.362	0.392	0.376	0.397	0.375	0.399	0.370	0.399	0.384	0.402	0.376	0.419	0.449	0.479
	192	0.396	0.412	0.405	0.416	0.413	0.421	0.436	0.429	0.420	0.448	0.534	0.504	0.538	0.504
ETTh1	336	0.427	0.422	0.439	0.443	0.422	0.436	0.491	0.469	0.459	0.465	0.588	0.535	0.574	0.521
	720	0.441	0.455	0.472	0.490	0.447	0.466	0.521	0.500	0.506	0.507	0.643	0.616	0.562	0.535
	avg	0.406	0.418	0.422	0.437	0.413	0.430	0.458	0.450	0.440	0.460	0.570	0.537	0.542	0.510
	96	0.262	0.320	0.289	0.353	0.274	0.336	0.340	0.374	0.358	0.397	0.476	0.458	0.340	0.391
	192	0.331	0.373	0.383	0.418	0.339	0.379	0.402	0.414	0.429	0.439	0.512	0.493	0.430	0.439
ETTh2	336	0.358	0.403	0.448	0.465	0.329	0.380	0.452	0.452	0.496	0.487	0.552	0.551	0.485	0.479
	720	0.369	0.411	0.605	0.551	0.379	0.422	0.462	0.468	0.463	0.474	0.562	0.560	0.500	0.497
	avg	0.330	0.376	0.431	0.446	0.330	0.379	0.414	0.427	0.439	0.452	0.602	0.543	0.450	0.459
	96	0.272	0.336	0.299	0.343	0.290	0.342	0.338	0.375	0.379	0.419	0.386	0.398	0.375	0.398
	192	0.310	0.357	0.335	0.365	0.332	0.369	0.374	0.387	0.426	0.441	0.459	0.444	0.408	0.410
ETTm1	336	0.351	0.382	0.369	0.386	0.366	0.392	0.410	0.411	0.445	0.459	0.495	0.464	0.435	0.428
	720	0.380	0.409	0.425	0.421	0.416	0.420	0.478	0.450	0.543	0.490	0.585	0.516	0.499	0.462
	avg	0.328	0.371	0.357	0.378	0.351	0.380	0.400	0.406	0.448	0.452	0.481	0.456	0.429	0.425
	96	0.163	0.254	0.167	0.269	0.165	0.255	0.187	0.267	0.203	0.287	0.192	0.274	0.189	0.280
	192	0.218	0.290	0.224	0.303	0.220	0.292	0.249	0.309	0.269	0.328	0.280	0.339	0.253	0.319
ETTm2	336	0.271	0.328	0.281	0.342	0.274	0.329	0.321	0.351	0.325	0.366	0.334	0.361	0.314	0.357
	720	0.356	0.382	0.397	0.421	0.362	0.385	0.408	0.403	0.421	0.415	0.417	0.413	0.414	0.413
	avg	0.252	0.627	0.267	0.333	0.255	0.315	0.291	0.333	0.305	0.349	0.371	0.306	0.347	0.293
	96	0.146	0.196	0.176	0.237	0.149	0.198	0.172	0.220	0.217	0.296	0.173	0.223	0.197	0.281
	192	0.193	0.236	0.220	0.282	0.194	0.241	0.219	0.261	0.276	0.336	0.245	0.285	0.237	0.312
Weather	336	0.239	0.240	0.265	0.319	0.245	0.282	0.280	0.306	0.339	0.380	0.321	0.338	0.298	0.353
	720	0.301	0.316	0.333	0.362	0.314	0.334	0.365	0.359	0.403	0.428	0.414	0.410	0.352	0.288
	avg	0.219	0.247	0.248	0.300	0.225	0.264	0.259	0.287	0.309	0.360	0.288	0.314	0.271	0.334
	96	0.130	0.219	0.140	0.237	0.129	0.222	0.168	0.272	0.193	0.308	0.169	0.273	0.187	0.304
	192	0.154	0.243	0.153	0.249	0.157	0.240	0.184	0.289	0.201	0.315	0.182	0.286	0.199	0.315
Electricity	336	0.158	0.245	0.169	0.267	0.163	0.259	0.198	0.300	0.214	0.329	0.200	0.304	0.212	0.329
	720	0.190	0.294	0.203	0.301	0.197	0.290	0.220	0.320	0.246	0.355	0.222	0.321	0.233	0.345
	avg	0.158	0.251	0.166	0.263	0.161	0.252	0.192	0.295	0.214	0.327	0.193	0.296	0.208	0.323
	96	0.361	0.248	0.410	0.282	0.360	0.249	0.593	0.321	0.587	0.366	0.612	0.338	0.607	0.392
FD 66	192	0.376	0.250	0.423	0.287	0.379	0.256	0.617	0.336	0.604	0.373	0.613	0.340	0.621	0.399
Traffic	336	0.382	0.268	0.436	0.296	0.392	0.264	0.629	0.336	0.621	0.383	0.618	0.328	0.622	0.396
	720	0.426	0.281	0.466	0.315	0.432	0.286	0.640	0.350	0.626	0.382	0.653	0.355	0.632	0.396
	avg	0.386	0.261	0.433	0.295	0.390	0.263	0.620	0.336	0.610	0.376	0.628	0.379	0.624	0.340
	24	1.301	0.739	2.215	1.081	1.319	0.754	2.317	0.934	3.228	1.260	2.294	0.945	2.527	1.020
** *	36	1.409	0.824	1.963	0.963	1.430	0.834	1.972	0.920	2.679	1.080	1.825	0.848	2.615	1.007
ILI	48	1.520	0.807	2.130	1.024	1.553	0.815	2.238	0.940	2.622	1.078	2.010	0.900	2.359	0.972
	60	1.553	0.852	2.368	1.096	1.520	0.788	2.027	0.928	2.857	1.157	2.178	0.963	2.487	1.016
	avg	1.439	0.805	2.169	1.041	1.443	0.797	2.139	0.931	2.847	1.144	2.077	0.914	2.497	1.004

Table 2: Multivariate long-term time-series forecasting: lower values indicate better performance. Forecasting horizons are $h \in \{24, 36, 48, 60\}$ for ILI and $h \in \{96, 192, 336, 720\}$ for the rest.

Signature Feature Extraction: Table 6 shows the entropy of extracted features by baseline (\mathbf{h}_t) , reservoir (\mathbf{z}_t) , and RT (\mathbf{f}_t) . Our RT model extracts more informative features than the baseline

	-41 4-	R	T	TIME	-LLM	GPT	Γ2TS	Mada		F	RT	TIME	-LLM	GPT	T2TS
IVI	ethods	(O	urs)	(20	24)	(20)24)	Meth	oas	(O	urs)	(20	24)	(20	24)
M	Ietric	MSE	MAE	MSE	MAE	MSE	MAE	Meti	ic	MSE	MAE	MSE	MAE	MSE	MAE
	96	0.361	0.386	0.362	0.392	0.376	0.397		96	0.146	0.196	0.147	0.201	0.162	0.212
	192	0.396	0.412	0.398	0.418	0.416	0.418		192	0.193	0.236	0.189	0.234	0.204	0.248
ETTh1	336	0.427	0.422	0.4427	0.433	0.439	0.433	Weather	336	0.239	0.240	0.262	0.279	0.254	0.286
	720	0.441	0.455	0.442	0.457	0.477	0.456		720	0.301	0.316	0.300	0.316	0.326	0.337
	avg	0.408	0.423	0.408	0.423	0.465	0.455		avg	0.219	0.247	0.225	0.257	0.237	0.270
·	96	0.262	0.320	0.268	0.328	0.285	0.342		96	0.130	0.222	0.131	0.224	0.139	0.238
	192	0.331	0.373	0.329	0.375	0.354	0.389		192	0.154	0.243	0.152	0.241	0.153	0.251
ETTh2	336	0.358	0.403	0.368	0.409	0.373	0.407	Electricity	336	0.158	0.245	0.160	0.248	0.169	0.266
	720	0.369	0.411	0.372	0.420	0.406	0.441		720	0.190	0.294	0.192	0.298	0.206	0.297
	avg	0.330	0.376	0.334	0.383	0.381	0.412		avg	0.158	0.251	0.158	0.252	0.167	0.263
	96	0.272	0.336	0.272	0.334	0.292	0.346		96	0.361	0.248	0.362	0.248	0.388	0.282
	192	0.310	0.357	0.310	0.358	0.332	0.372		192	0.376	0.250	0.374	0.247	0.407	0.290
ETTm1	336	0.351	0.382	0.352	0.384	0.366	0.394	Traffic	336	0.382	0.268	0.385	0.271	0.412	0.294
	720	0.380	0.409	0.383	0.411	0.417	0.421		720	0.426	0.281	0.430	0.288	0.450	0.312
	avg	0.328	0.371	0.329	0.372	0.388	0.403		avg	0.386	0.261	0.388	0.264	0.414	0.294
	96	0.163	0.254	0.161	0.253	0.173	0.262		24	1.301	0.739	1.285	0.727	2.063	0.881
	192	0.218	0.290	0.219	0.293	0.229	0.301		36	1.409	0.824	1.404	0.814	1.868	0.892
ETTm2	336	0.271	0.328	0.271	0.329	0.286	0.341	ILI	48	1.520	0.807	1.523	0.807	1.790	0.884
	720	0.356	0.382	0.352	0.379	0.378	0.401		60	1.529	0.852	1.531	0.854	1.979	0.957
	avg	0.252	0.316	0.251	0.313	0.284	0.339		avg	1.439	0.805	1.435	0.801	1.925	0.903
Avg. Tra	aining Time	3.150 N	Minutes	55.41 N	Ainutes		Minutes	Avg. Train	ing Time	36.52	Minutes	510.21	Minutes	146.3 1	Minutes
Avg. Occ	cupied GPU	2.03	3 GB	74.42	2 GB	16.3	1 GB	Avg. Occup	ied GPU	2.11	0 GB	77.27	71 GB	17.68	80 GB

Table 3: Multivariate time-series forecasting (low chaos) comparison with pre-trained LLM model. 'Avg. Training Time' is the average training time for the model. 'Avg. Occupied GPU' is the average GPU memory usage for the model.

Method	Air Q		DV		DG	-	DI		BT	~ 1	-	AW	1	TR
Metric												F-Score		
Transformer														
RT (Ours)	70.58	9.040	6.181	1.893	28.79K	119.2	10.17	410.6	211.6	211.6	0.899	0.901	0.802	0.975

Table 4: Time series comparison (medium chaos) in MSE, MAE, Accuracy, and F-score with RT and baseline Transformer. 'Acc.' is the Accuracy.

Transformer model. Using the Shannon entropy to measure the information amount, our reservoir output features \mathbf{z}_t have higher entropy (more informative) than the embedding output features \mathbf{h}_t in the baseline Transformer. Combining both \mathbf{f}_t gives the highest entropy among them, demonstrating more information extraction with our RT. Details of the experiments are enclosed in the Appendix G.2.

Method	I	RT (Ours	5)		DLinear]	PatchTS7	Γ		Entro	ру	
Horizons	MGS	ECG	LA	MGS	ECG	LA	MGS	ECG	LA	Datasets	\mathbf{h}_t	\mathbf{z}_t	\mathbf{f}_t
50	0.173	0.301	0.313	0.204	0.321	0.356	0.179	0.297	0.310	ETTh1	1.011	1.966	2.331
100	0.185	0.314	0.331	0.225	0.343	0.370	0.186	0.315	0.313	ETTh2	0.993	1.892	2.015
500	0.206	0.341	0.359	0.240	0.371	0.389	0.209	0.347	0.360	ETTm1	0.816	2.056	2.831
1000	0.225	0.374	0.447	0.250	0.390	0.529	0.228	0.378	0.449	ETTm2	0.599	1.248	2.131

Table 5: MSE on three typical chaos datasets (high chaos).

Table 6: Feature entropy.

4.1 Ablation Analysis

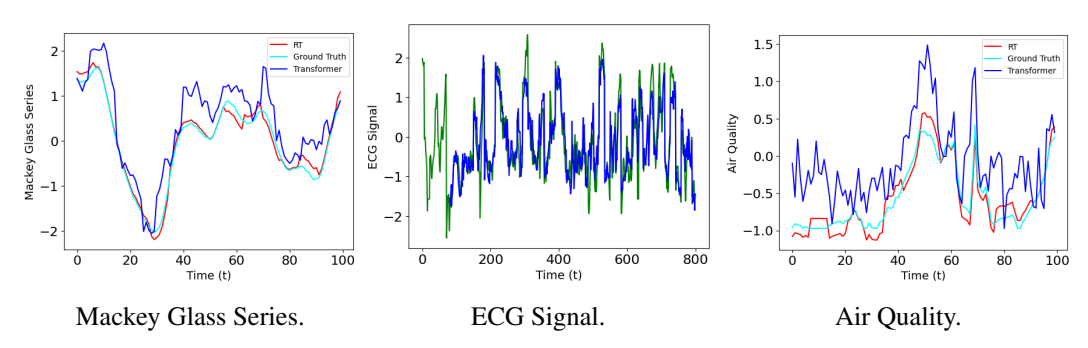


Figure 2: The figures represent chaotic dataset examples. The cyan line is ground truth; the red line is the prediction using RT; and the blue line is the prediction using Transformer.

Output Examples: Figure 1 (Right) and Figure 2 plots the examples from three datasets. We show that our RT method output is more close to the ground truth than the Transformer baseline.

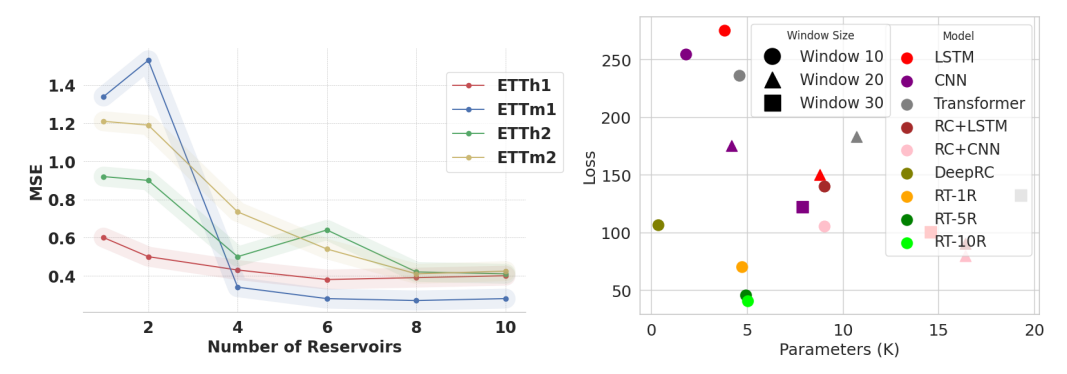


Figure 3: MSE vs. reservoir numbers. Fig

Figure 4: RT outperforms baselines with

Impact of Reservoir Count on Performance: Figure 3 illustrates the relationship between the number of ensembling reservoirs and system performance. Increasing the number of reservoirs improves the performance, leading to a reduction in loss until the loss converges for 10 reservoirs.

Model Parameter Size versus Loss: Conventional models require a large number of training parameters for long historical sequences. In contrast, RT only train a vector representation (i.e. readout) for the next time step without explicit conditioning on the entire history. Figure 4 illustrates that RT provides a better trade-off between the number of training parameters and loss.

Initialization	ĺ	ETTh1	<u> </u>	ETTh2		ETTm1	E	ΓTm2	V	Veather	<u> </u>	Traffic
IIIIIaiizatioii	NG	G	NG	G	NG	G	NG	G	NG	G	NG	G
Random	0.543	0.402	0.435	0.342	0.447	0.328	0.301	0.228	0.334	0.198	0.424	0.380
Zero	0.429	0.396	0.368	0.331	0.348	0.310	0.236	0.218	0.215	0.193	0.380	0.376
Constant	0.673	0.405	0.420	0.333	0.516	0.319	0.265	0.225	0.204	0.196	0.424	0.378
Normal	0.529	0.401	0.445	0.335	0.435	0.332	0.274	0.236	0.242	0.198	0.452	0.379
Uniform	0.432	0.399	0.395	0.331	0.401	0.314	0.232	0.219	0.200	0.195	0.401	0.375
p-value	0.249	$2.31 \cdot 10^{-6}$	0.049	$4.36 \cdot 10^{-5}$	0.120	$1.94 \cdot 10^{-4}$	0.226	$5 \cdot 10^{-3}$	0.436	$2.2 \cdot 10^{-5}$	0.187	$3.15 \cdot 10^{-5}$

Table 7: MSE on different initialization using single reservoir (NG) and group reservoirs (G). Group reservoir eliminates the prediction error sensitivity on the initialization.

Model	Memory (Cache) Footprint	Context Length	Model	Time Complexity	Seq. Ops.
Transformer-XL	$(d_{key} + d_{value}) \cdot H \cdot k \cdot ly$	$k \cdot ly$	Transformer	$O(T^2 \cdot d_{\epsilon})$	O(1)
Compressive Transformer	$d_{\epsilon} \cdot (c+T) \cdot ly$	$ (c \cdot r + k) \cdot ly $	PatchTST	$O((T/P)^2 \cdot d_{\epsilon})$	O(1)
Memorizing Transformers	$(d_{key} + d_{value}) \cdot H \cdot k \cdot T$	T	Informer	$O(T \cdot log(T) \cdot d_{\epsilon})$	O(1)
RMT	$d_{\epsilon} \cdot p \cdot ly \cdot 2$	T	Autoformer	$O(T \cdot log(T) \cdot d_{\epsilon})$	O(1)
AutoCompressors	$d_{\epsilon} \cdot p \cdot (v+1) \cdot ly$	T	Reformer	$O(T \cdot log(T) \cdot d_{\epsilon})$	O(1)
Infini-Transformers	$d_{key} \cdot (d_{value} + 1) \cdot H \cdot ly$	T	RNN	$O(T \cdot d_{\epsilon}^2)$	O(T)
Reservoir	N_r^2	T	Reservoir	$O(T \cdot N_r^2)$	O(T)
RT (Ours)	$N_r^2 \cdot L$	T	RT (Ours)	$O(T \cdot k^2 \cdot d_{\epsilon})$	O(T)

Table 8: Comparison of memory (cache) footprint and time complexity.

Initialization Comparison: Table 7 shows how different initialization affects the performance for each of the datasets. We compute the the p-value to see whether the variation in performance due to different initialization is significant when comparing a single reservoir (Non-Group denoted with 'NG') with an group reservoir (Group denoted with 'G'). We use the combined mean for each dataset as the population mean to compute the p-values. We observe significant differences for all the datasets for only the Non-Group experiments.

Complexity Comparison: Table 8 shows the memory (cache) footprint and time complexity of different models. 'Seq. Ops.' is the 'Sequential Operations', and the notations are as follows. N_r is the reservoir state; L is the number of reservoirs in the group reservoir; k is the short-term context window length; T is the long-term context total input length; t is the number of layers; t is the number of attention heads; t is the Compressive Transformer memory size; t is the compression ratio; t is the number of soft-prompt summary vectors; t is the summary vector accumulation steps; t is the kernel size; t is the patch size; t is the embedding model dimension; t is the dimension of keys in attention; and t is the dimension of values in attention. RT maintains a constant memory

complexity of $N_r^2 \cdot L$, and the time complexity is linear regarding total input length. Additionally, RT updates its memory with each new input, resulting in retrieval and update occurring once per input. Other methods like Transformer-XL [Dai et al., 2019], Compressive Transformer [Rae et al., 2019], Memorizing Transformers [Wu et al., 2022b], RMT [Bulatov et al., 2022], and AutoCompressors [Chevalier et al., 2023] do not have constant memory usage; it depends on the total input segment length N and still exhibits a large context-memory complexity. Furthermore, RMT [Bulatov et al., 2022] and AutoCompressors [Chevalier et al., 2023] allow for a potentially infinite context length since they compress the input into summary vectors and then pass them as extra soft-prompt inputs for the subsequent segments. However, in practice, the success of those techniques highly depends on the size of soft-prompt vectors [Munkhdalai et al., 2024].

5 Related Work

Time-series prediction using machine learning approaches has been investigated in the last decade using CNN, WNN, FNN, LSTM, etc. [Ramadevi and Bingi, 2022, Sangiorgio and Dercole, 2020, Karasu and Altan, 2022, Sahoo et al., 2019, PaperwithCodes, 2022] on datasets with chaotic properties. Recently, Transformer-based solutions have shown success for long-term time series forecasting (LTSF) [Mohammadi Farsani and Pazouki, 2020, Huang et al., 2019]. Recently, researchers have also used various methods to improve long-term time series forecasting [Zhou et al., 2022, 2021, Wu et al., 2021]. Nonetheless, the Transformer is expensive in terms of quadratic time and space complexity of the input length. Important works have been proposed in improving Transformer architectures and their complexity in long context in various ways, however, compressing the long input sequence into fixed length often misses the dependency of the temporal events.

Researchers have also shown how using pre-trained LLMs for time-series data improves performance compared to training from scratch [Jin et al., 2023, Chang et al., 2024, Huang, 2024, Munkhdalai et al., 2024]. de Zarzà et al. [2023] used a combination of LLMs (LLaMA-2 and Zephyr-7b- α) along with Multimodal LLM (LLaVA) for time-series forecasting. However, there is still a restriction on the input length due to the complexity of the neural network models. Note that we will experimentally compare with [Munkhdalai et al., 2024] once their code releases.

Reservoir networks with their simplified training and superior performance for time-series forecasting compared to the traditional models, including time-series kernels, feed-forward networks, and RNN models, has been well documented. Researchers have also compared different types of reservoir networks for chaotic time-series data [Bo et al., 2020]. However, the reservoir network fails to effectively handle long context time series data within fixed-size reservoir [Lukoševičius and Jaeger, 2009, Kim and King, 2020, Mansoor et al., 2021, Bianchi et al., 2020]. We have introduced reservoir computing to solve the input length problem. A concept of reservoir Transformer [Shen et al., 2020, Gauthier et al., 2021] was introduced by interspersing the reservoir layers into the regular Transformer layers and showing improvements in wall-clock compute time. These models improve the training efficiency by using parallelization of time-series methods [Bollt, 2021]. However, such integration will reduce the feature extraction power of both reservoirs in the long sequences and Transformer in short sequences. We do not combine the reservoir and Transformer linearly but in a non-linear way and receive significant improvements over all previous methods in time-series prediction, including chaotic prediction. Additionally, there has been research on using ensemble of models for time-series prediction. Researchers have proposed ensemble methods [Feng et al., 2019] that combine multiple hybrid models using wavelet transform for chaotic time-series prediction and achieved improved performance on several chaotic systems. [Tang et al., 2020, Oliveira and Torgo, 2015, Bertsimas and Boussioux, 2023] proposed an ensemble method that combines multiple deep-learning models for time-series prediction and showed improved performance on several datasets. In our work, we propose a novel method to ensemble multiple reservoir networks and combine them with Transformer architecture, contributing to improved performance in time-series prediction.

6 Conclusion

Our RT has the unique advantage of handling any input length and producing robust prediction outputs. Thus, it is ideal for time-series forecasting, including event prediction in chaos. We introduce nonlinear readouts to our Reservoir Transformer that outperform state-of-the-art models in terms of accuracy, keeping reasonable complexity in space and time. Furthermore, we testify to long-horizon

forecasting and show that RT makes the far-horizon prediction less sensitive to initialization. This research direction has the potential for succession works by integrating chaotic analysis, deep neural networks, and reservoir computing to understand and predict our environments better.

References

- Zonghua Liu. Nonlinear time series: Computations and applications, 2010.
- Dominic Jordan and Peter Smith. *Nonlinear ordinary differential equations: an introduction for scientists and engineers*. OUP Oxford, 2007.
- Xiang Wu, Xujun Yang, Qiankun Song, and Chuandong Li. Generalized lyapunov stability theory of continuous-time and discrete-time nonlinear distributed-order systems and its application to boundedness and attractiveness for networks models. *Communications in Nonlinear Science and Numerical Simulation*, 128:107664, 2024.
- Ailing Zeng, Muxi Chen, Lei Zhang, and Qiang Xu. Are transformers effective for time series forecasting? *arXiv preprint arXiv:2205.13504*, 2022.
- Ashish Vaswani, Noam Shazeer, Niki Parmar, Jakob Uszkoreit, Llion Jones, Aidan N Gomez, Łukasz Kaiser, and Illia Polosukhin. Attention is all you need. *Advances in neural information processing systems*, 30, 2017.
- Amanda Bertsch, Uri Alon, Graham Neubig, and Matthew R Gormley. Unlimiformer: Long-range transformers with unlimited length input. *arXiv preprint arXiv:2305.01625*, 2023.
- Yi Tay, Mostafa Dehghani, Dara Bahri, and Donald Metzler. Efficient transformers: A survey. ACM Computing Surveys, 55(6):1–28, 2022.
- Nikita Kitaev, Łukasz Kaiser, and Anselm Levskaya. Reformer: The efficient transformer. *arXiv* preprint arXiv:2001.04451, 2020.
- Erik Bollt. On explaining the surprising success of reservoir computing forecaster of chaos? the universal machine learning dynamical system with contrast to var and dmd. *Chaos: An Interdisciplinary Journal of Nonlinear Science*, 31(1), 2021.
- Ming Jin, Shiyu Wang, Lintao Ma, Zhixuan Chu, James Y. Zhang, Xiaoming Shi, Pin-Yu Chen, Yuxuan Liang, Yuan-Fang Li, Shirui Pan, and Qingsong Wen. Time-LLM: Time series forecasting by reprogramming large language models. In *The Twelfth International Conference on Learning Representations*, 2024. URL https://openreview.net/forum?id=Unb5CVPtae.
- Yuqi Nie, Nam H Nguyen, Phanwadee Sinthong, and Jayant Kalagnanam. A time series is worth 64 words: Long-term forecasting with transformers. *arXiv preprint arXiv:2211.14730*, 2022.
- Iz Beltagy, Matthew E Peters, and Arman Cohan. Longformer: The long-document transformer. *arXiv* preprint arXiv:2004.05150, 2020.
- Taesung Kim, Jinhee Kim, Yunwon Tae, Cheonbok Park, Jang-Ho Choi, and Jaegul Choo. Reversible instance normalization for accurate time-series forecasting against distribution shift. In *International Conference on Learning Representations*, 2021.
- Haoyi Zhou, Shanghang Zhang, Jieqi Peng, Shuai Zhang, Jianxin Li, Hui Xiong, and Wancai Zhang. Informer: Beyond efficient transformer for long sequence time-series forecasting. In *Proceedings of the AAAI conference on artificial intelligence*, pages 11106–11115, 2021.
- Haixu Wu, Jiehui Xu, Jianmin Wang, and Mingsheng Long. Autoformer: Decomposition transformers with auto-correlation for long-term series forecasting. *Advances in Neural Information Processing Systems*, 34:22419–22430, 2021.
- Shizhan Liu, Hang Yu, Cong Liao, Jianguo Li, Weiyao Lin, Alex X Liu, and Schahram Dustdar. Pyraformer: Low-complexity pyramidal attention for long-range time series modeling and forecasting. In *International Conference on Learning Representations*, 2021.

- Yunhao Zhang and Junchi Yan. Crossformer: Transformer utilizing cross-dimension dependency for multivariate time series forecasting. In *The eleventh international conference on learning representations*, 2022.
- Robin Rombach, Andreas Blattmann, Dominik Lorenz, Patrick Esser, and Björn Ommer. High-resolution image synthesis with latent diffusion models. In *Proceedings of the IEEE/CVF conference on computer vision and pattern recognition*, pages 10684–10695, 2022.
- Xi Wei, Tianzhu Zhang, Yan Li, Yongdong Zhang, and Feng Wu. Multi-modality cross attention network for image and sentence matching. In *Proceedings of the IEEE/CVF conference on computer vision and pattern recognition*, pages 10941–10950, 2020.
- Herbert Jaeger and Harald Haas. Harnessing nonlinearity: Predicting chaotic systems and saving energy in wireless communication. *science*, 304(5667):78–80, 2004.
- Mantas Lukoševičius and Herbert Jaeger. Reservoir computing approaches to recurrent neural network training. *Computer science review*, 3(3):127–149, 2009.
- David Verstraeten, Benjamin Schrauwen, Michiel d'Haene, and Dirk Stroobandt. An experimental unification of reservoir computing methods. *Neural networks*, 20(3):391–403, 2007.
- Peter Tiňo, Barbara Hammer, and Mikael Bodén. Markovian bias of neural-based architectures with feedback connections. In *Perspectives of neural-symbolic integration*, pages 95–133. Springer, 2007.
- Herbert Jaeger, Mantas Lukoševičius, Dan Popovici, and Udo Siewert. Optimization and applications of echo state networks with leaky-integrator neurons. *Neural networks*, 20(3):335–352, 2007.
- Fabian Triefenbach and Jean-Pierre Martens. Can non-linear readout nodes enhance the performance of reservoir-based speech recognizers? In 2011 First International Conference on Informatics and Computational Intelligence, pages 262–267. IEEE, 2011.
- Claudio Gallicchio, Alessio Micheli, and Luca Pedrelli. Deep reservoir computing: A critical experimental analysis. *Neurocomputing*, 268:87–99, 2017.
- Peter Shaw, Jakob Uszkoreit, and Ashish Vaswani. Self-attention with relative position representations. *arXiv preprint arXiv:1803.02155*, 2018.
- Daniel J Gauthier, Erik Bollt, Aaron Griffith, and Wendson AS Barbosa. Next generation reservoir computing. *Nature communications*, 12(1):1–8, 2021.
- Gregory P Meyer. An alternative probabilistic interpretation of the huber loss. In *Proceedings of the ieee/cvf conference on computer vision and pattern recognition*, pages 5261–5269, 2021.
- Ailing Zeng, Muxi Chen, Lei Zhang, and Qiang Xu. Are transformers effective for time series forecasting? In *Proceedings of the AAAI conference on artificial intelligence*, volume 37, pages 11121–11128, 2023.
- Haixu Wu, Tengge Hu, Yong Liu, Hang Zhou, Jianmin Wang, and Mingsheng Long. Timesnet: Temporal 2d-variation modeling for general time series analysis. In *The eleventh international conference on learning representations*, 2022a.
- Tian Zhou, Ziqing Ma, Qingsong Wen, Xue Wang, Liang Sun, and Rong Jin. Fedformer: Frequency enhanced decomposed transformer for long-term series forecasting. *arXiv preprint arXiv:2201.12740*, 2022.
- Yong Liu, Haixu Wu, Jianmin Wang, and Mingsheng Long. Non-stationary transformers: Exploring the stationarity in time series forecasting. *Advances in Neural Information Processing Systems*, 35: 9881–9893, 2022.
- Gerald Woo, Chenghao Liu, Doyen Sahoo, Akshat Kumar, and Steven Hoi. Etsformer: Exponential smoothing transformers for time-series forecasting. *arXiv preprint arXiv:2202.01381*, 2022.

- David Campos, Miao Zhang, Bin Yang, Tung Kieu, Chenjuan Guo, and Christian S Jensen. Lightts: Lightweight time series classification with adaptive ensemble distillation. *Proceedings of the ACM on Management of Data*, 1(2):1–27, 2023.
- Minghao Chen, Houwen Peng, Jianlong Fu, and Haibin Ling. Autoformer: Searching transformers for visual recognition. In *Proceedings of the IEEE/CVF international conference on computer vision*, pages 12270–12280, 2021.
- Tian Zhou, Peisong Niu, Liang Sun, Rong Jin, et al. One fits all: Power general time series analysis by pretrained lm. *Advances in neural information processing systems*, 36, 2024.
- Radim Pánis, Martin Kološ, and Zdeněk Stuchlík. Detection of chaotic behavior in time series. *arXiv* preprint arXiv:2012.06671, 2020.
- Z Dai, Z Yang, Y Yang, J Carbonell, Q Le, and R Transformer-XL Salakhutdinov. Attentive language models beyond a fixed-length context. 2019. *arXiv preprint arXiv:1901.02860*, 2019.
- Jack W Rae, Anna Potapenko, Siddhant M Jayakumar, and Timothy P Lillicrap. Compressive transformers for long-range sequence modelling. *arXiv preprint arXiv:1911.05507*, 2019.
- Yuhuai Wu, Markus N Rabe, DeLesley Hutchins, and Christian Szegedy. Memorizing transformers. *arXiv preprint arXiv:2203.08913*, 2022b.
- Aydar Bulatov, Yury Kuratov, and Mikhail Burtsev. Recurrent memory transformer. *Advances in Neural Information Processing Systems*, 35:11079–11091, 2022.
- Alexis Chevalier, Alexander Wettig, Anirudh Ajith, and Danqi Chen. Adapting language models to compress contexts. *arXiv preprint arXiv:2305.14788*, 2023.
- Tsendsuren Munkhdalai, Manaal Faruqui, and Siddharth Gopal. Leave no context behind: Efficient infinite context transformers with infini-attention. *arXiv* preprint arXiv:2404.07143, 2024.
- Bhukya Ramadevi and Kishore Bingi. Chaotic time series forecasting approaches using machine learning techniques: A review. *Symmetry*, 14(5):955, 2022.
- Matteo Sangiorgio and Fabio Dercole. Robustness of lstm neural networks for multi-step forecasting of chaotic time series. *Chaos, Solitons & Fractals*, 139:110045, 2020.
- Seçkin Karasu and Aytaç Altan. Crude oil time series prediction model based on 1stm network with chaotic henry gas solubility optimization. *Energy*, 242:122964, 2022.
- Bibhuti Bhusan Sahoo, Ramakar Jha, Anshuman Singh, and Deepak Kumar. Long short-term memory (lstm) recurrent neural network for low-flow hydrological time series forecasting. *Acta Geophysica*, 67(5):1471–1481, 2019.
- PaperwithCodes. Leaderboards of time series forecasting, 2022.
- R Mohammadi Farsani and Ehsan Pazouki. A transformer self-attention model for time series forecasting. *Journal of Electrical and Computer Engineering Innovations (JECEI)*, 9(1):1–10, 2020.
- Siteng Huang, Donglin Wang, Xuehan Wu, and Ao Tang. Dsanet: Dual self-attention network for multivariate time series forecasting. In *Proceedings of the 28th ACM international conference on information and knowledge management*, pages 2129–2132, 2019.
- Ming Jin, Shiyu Wang, Lintao Ma, Zhixuan Chu, James Y Zhang, Xiaoming Shi, Pin-Yu Chen, Yuxuan Liang, Yuan-Fang Li, Shirui Pan, et al. Time-llm: Time series forecasting by reprogramming large language models. *arXiv preprint arXiv:2310.01728*, 2023.
- Ching Chang, Wei-Yao Wang, Wen-Chih Peng, and Tien-Fu Chen. Llm4ts: Aligning pre-trained llms as data-efficient time-series forecasters. https://arxiv.org/abs/2308.08469, 2024.
- Xiannan Huang. Enhancing traffic prediction with textual data using large language models. *arXiv* preprint arXiv:2405.06719, 2024.

- I de Zarzà, J de Curtò, Gemma Roig, and Carlos T Calafate. Llm multimodal traffic accident forecasting. *Sensors*, 23(22):9225, 2023.
- Ying-Chun Bo, Ping Wang, and Xin Zhang. An asynchronously deep reservoir computing for predicting chaotic time series. *Applied Soft Computing*, 95:106530, 2020.
- Taehwan Kim and Brian R King. Time series prediction using deep echo state networks. *Neural Computing and Applications*, 32(23):17769–17787, 2020.
- Muhammad Mansoor, Francesco Grimaccia, Sonia Leva, and Marco Mussetta. Comparison of echo state network and feed-forward neural networks in electrical load forecasting for demand response programs. *Mathematics and Computers in Simulation*, 184:282–293, 2021.
- Filippo Maria Bianchi, Simone Scardapane, Sigurd Løkse, and Robert Jenssen. Reservoir computing approaches for representation and classification of multivariate time series. *IEEE transactions on neural networks and learning systems*, 32(5):2169–2179, 2020.
- Sheng Shen, Alexei Baevski, Ari S Morcos, Kurt Keutzer, Michael Auli, and Douwe Kiela. Reservoir transformers. *arXiv preprint arXiv:2012.15045*, 2020.
- Tian Feng, Shuying Yang, and Feng Han. Chaotic time series prediction using wavelet transform and multi-model hybrid method. *Journal of Vibroengineering*, 21(7):1983–1999, 2019.
- Li-Hong Tang, Yu-Long Bai, Jie Yang, and Ya-Ni Lu. A hybrid prediction method based on empirical mode decomposition and multiple model fusion for chaotic time series. *Chaos, Solitons & Fractals*, 141:110366, 2020.
- Mariana Oliveira and Luis Torgo. Ensembles for time series forecasting. In *Asian Conference on Machine Learning*, pages 360–370. PMLR, 2015.
- Dimitris Bertsimas and Leonard Boussioux. Ensemble modeling for time series forecasting: an adaptive robust optimization approach. *arXiv preprint arXiv:2304.04308*, 2023.
- Shiyang Li, Xiaoyong Jin, Yao Xuan, Xiyou Zhou, Wenhu Chen, Yu-Xiang Wang, and Xifeng Yan. Enhancing the locality and breaking the memory bottleneck of transformer on time series forecasting. *Advances in neural information processing systems*, 32, 2019.
- Andrea Cini, Ivan Marisca, and Cesare Alippi. Filling the gaps: Multivariate time series imputation by graph neural networks. *arXiv* preprint arXiv:2108.00298, 2021.
- Wei Cao, Dong Wang, Jian Li, Hao Zhou, Lei Li, and Yitan Li. Brits: Bidirectional recurrent imputation for time series. *Advances in neural information processing systems*, 31, 2018.
- Xiuwen Yi, Yu Zheng, Junbo Zhang, and Tianrui Li. St-mvl: filling missing values in geo-sensory time series data. In *Proceedings of the 25th International Joint Conference on Artificial Intelligence*, 2016.
- Jinsung Yoon, William R Zame, and Mihaela van der Schaar. Estimating missing data in temporal data streams using multi-directional recurrent neural networks. *IEEE Transactions on Biomedical Engineering*, 66(5):1477–1490, 2018.
- Steffen Moritz and Thomas Bartz-Beielstein. imputets: time series missing value imputation in r. *R J.*, 9(1):207, 2017.

A Dataset and Parameter Configuration

In this subsection, we outline the approach taken for dataset partitioning and parameter selection within our research framework.

Dataset Partitioning: For the datasets ETTh1, ETTh2, ETTm1, ETTm2, Traffic, Weather, and ILI, we adopted the data preparation settings outlined by [Zeng et al., 2023]. For other datasets, we divided the data sequentially into three distinct sets: training (70%), validation (10%), and testing (20%). This division strategy facilitates efficient training, validation, and testing of models.

Tools and Hardware: We have used Pytorch and Huggingface libraries to implement our framework. All the experiments were carried out on a single Nvidia RTX-4090 or Tesla H100 GPU.

Model Parameters: The configuration of model parameters plays a crucial role in experiments. For the Transformer architecture, we employ four Transformer blocks, each comprising 12 multi-head attention mechanisms with a total of 12 attention layers. In the case of the Feedforward Neural Network (FNN), we utilize hidden layers containing 64 units each.

Within the network architecture, dropout is employed as a regularization technique. Specifically, a dropout rate of 0.4 is applied to the hidden layers, while a rate of 0.1 is used for the reservoir network. Additionally, dropout with a rate of 0.2 is integrated into the attention network.

Furthermore, the reservoir state size varies between 200 and 300 units across different ensembling reservoirs. To introduce diversity in the ensembling process, spectral radius values range from 0.5 to 0.9 for different reservoirs, accompanied by leaky units with values ranging from 0.2 to 0.6.

Finally, a learning rate of 1×10^{-5} is adopted to facilitate the training process and achieve optimal convergence.

By meticulously configuring these parameters, we aim to attain a comprehensive understanding of the model's performance across various experimental setups.

Evaluation metric: In order to analyze the performance and evaluation of the proposed work, Mean Squared Error (MSE), and Mean Absolute Error (MAE) has been used for regression. The MSE is a quantification of the mean squared difference between the actual and predicted values. The minimum difference, the better the model's performance. On the other hand, MAE is a quantification of the mean difference between the actual and predicted values. As like as MSE, the minimum score of MAE, the better the model's performance. For classification tasks, we have used Accuracy and F1 score metrics.

Dataset Description:

- ETTh (Electricity Transformer Temperature hourly-level): The ETTh dataset presents a comprehensive collection of transformer temperature and load data, recorded at an hourly granularity, covering the period from July 2016 to July 2018. The dataset has been meticulously organized to encompass hourly measurements of seven vital attributes related to oil and load characteristics for electricity transformers. These incorporated features provide a valuable resource for researchers to glean insights into the temporal behavior of transformers.
 - For the ETTh1 subset of the dataset, our model architecture entails the utilization of reservoir units ranging in size from 20 to 50, coupled with an ensemble comprising five distinct reservoirs. The attention mechanism deployed in this context employs a configuration of 15 attention heads, each possessing a dimension of 10 for both query and key components.
 - Likewise, for the ETTh2 subset, our approach involves employing a total of seven ensemble reservoirs, each incorporating reservoir units spanning from 20 to 50 in size. The remaining parameters for this subset remain consistent with the configuration established for ETTh1.
- ETTm (Electricity Transformer Temperature 15-minute-level): The ETTm dataset offers a heightened level of detail and granularity by capturing measurements at intervals as fine as 15 minutes. Similar to the ETTh dataset, ETTm spans the timeframe from July 2016 to July 2018. This dataset retains the same seven pivotal oil and load attributes for electricity transformers as in the ETTh dataset; however, the key distinction lies in its higher temporal resolution. This heightened level of temporal granularity holds the potential to unveil subtler patterns and intricacies in the behavior of transformers.

In the context of model architecture, the configuration adopted for the ETTm dataset involves the use of ensemble reservoirs. Specifically, for the ETTm1 subset, an ensemble of seven reservoirs is employed, while for the ETTm2 subset, an ensemble of six reservoirs is utilized. This distinctive architectural setup is designed to harness the increased temporal resolution of the ETTm dataset, enabling the model to capture and interpret the finer nuances within the transformer data.

- Exchange-Rate This dataset includes the daily exchange rates for eight foreign countries: Australia, Britain, Canada, Switzerland, China, Japan, New Zealand, and Singapore. This data ranges from the year 1990 to 2016. To analyze this information, we are using 15 reservoirs, which are a specific type of model to help us understand and predict changes in these exchange rates.
- AQI (Air Quality): The AQI dataset encompasses a collection of recordings pertaining to various air quality indices, sourced from 437 monitoring stations strategically positioned across 43 cities in China. Specifically, our analysis focuses solely on the PM2.5 pollutant for this study. Notably, previous research efforts in the realm of imputation have concentrated on a truncated rendition of this dataset, which comprises data from 36 sensors.

For our investigation, we leverage 15 ensemble reservoirs as the architectural foundation for this dataset. This ensemble configuration is tailored to the distinctive characteristics and complexities inherent in the AQI data. By deploying this setup, we endeavor to enhance our capacity to effectively address the intricate imputation challenges associated with the AQI dataset.

• Daily Website visitors: ¹The dataset pertinent to daily website visitors provides a comprehensive record of time series data spanning five years. This dataset encapsulates diverse metrics of traffic associated with statistical forecasting teaching notes. The variables encompass daily counts encompassing page loads, unique visitors, first-time visitors, and returning visitors to an academic teaching notes website. The dataset comprises 2167 rows, covering the timeline from September 14, 2014, to August 19, 2020.

From this array of variables, our specific focus centers on the 'first-time visitors,' which we have identified as the target variable within the context of a regression problem. By delving into this specific variable, we aim to uncover insights regarding the behavior of new visitors to the website and its associated dynamics.

In terms of the model architecture employed for this dataset, we have constructed a configuration centered around 12 ensemble reservoirs. This architectural choice reflects the dataset's intricacies and the requirement for an approach that can effectively capture the underlying patterns and variations within the daily website visitor data

• Daily Gold Price: ² The dataset pertaining to daily gold prices offers an extensive collection of time series data encompassing a span of five years. This dataset encapsulates a range of metrics pertaining to gold price dynamics. The variables included cover daily measurements related to various aspects of gold pricing. The dataset consists of 2167 rows, covering the time period from September 14, 2014, to August 19, 2020.

The primary objective in this analysis is regression, wherein we seek to model relationships and predict outcomes based on the available variables. Specifically, we are interested in predicting the daily gold price based on the given set of features.

In terms of the architectural setup for this dataset, we have established a model configuration that employs 10 ensemble reservoirs. This choice is rooted in the need to effectively capture the nuances and trends inherent in the daily gold price data. By employing this ensemble-based approach, we aim to enhance the model's capacity to discern patterns and fluctuations within the gold price time series.

• **Daily Demand Forecasting Orders:** ³ This is a regression dataset that was collected during 60 days, this is a real database of a Brazilian company of large logistics. Twelve predictive attributes and a target that is considered a non-urgent order. We used 17 ensemble reservoirs for this dataset.

¹https://www.kaggle.com/datasets/bobnau/daily-website-visitors

²https://www.kaggle.com/datasets/nisargchodavadiya/daily-gold-price-20152021-time-series

³https://archive.ics.uci.edu/dataset/409/dailydemandforecastingorders

Algorithm 1 Training algorithm of Deep Reservoir Computing

```
Require: \mathbf{u}_{1:T}, a Transformer model \mathbb{M}(.), a groups reservoirs \mathcal{R}(.), an embedding function \epsilon(.)
Ensure: Initialization \mathbb{M}(.) and \mathcal{R}(.) with parameters
    while epoch < epochs do
         for t \leftarrow k to T do
               \mathbf{h}_t = \epsilon(\mathbf{u}_{t-k:t})
                                                                                                      ▶ Embedding the time input(3.1)
               \mathbf{z}_t = \mathcal{R}(\mathbf{h}_t)
                                                                 ▶ Readout from Group reservoir (3.2, 3.3, 3.4, 3.5, 3.6)
               \mathbf{f}_t = (1 - \kappa)\mathbf{z}_t \uplus \kappa \mathbf{h}_t
                                                                                                                       ▷ Concatenation (3.7)
               \hat{\mathbf{u}}_{t+1:t+\tau} \leftarrow \mathbb{M}(\mathbf{f}_t)
         end for
         loss \leftarrow \mathcal{L}(\mathbf{u}_{t+1:t+\tau}, \hat{\mathbf{u}}_{t+1:t+\tau})
                                                                                                                    ▷ Calculating loss (3.8)
         update parameters
   end while
```

- **Bitcoin Historical Dataset (BTC):** ⁴ The dataset used in this research contains the historical price data of Bitcoin from its inception in 2009 to the present. It includes key metrics such as daily opening and closing prices, trading volumes, and market capitalizations. This comprehensive dataset captures Bitcoin's significant fluctuations and trends, reflecting major milestones and market influences. It serves as an essential tool for analyzing patterns, understanding price behaviors, and predicting future movements in the cryptocurrency market. We used 10 ensemble reservoirs for this dataset.
- **Absenteeism at Work:** ⁵ The dataset focusing on absenteeism at work is sourced from the UCI repository, specifically the "Absenteeism at work" dataset. In our analysis, the dataset has been utilized for classification purposes, specifically targeting the classification of individuals as social drinkers. The dataset comprises 21 attributes and encompasses a total of 740 records. These records pertain to instances where individuals were absent from work, and the data collection spans the period from January 2008 to December 2016.

Within the scope of this analysis, the primary objective is classification, wherein we endeavor to categorize individuals as either social drinkers or non-social drinkers based on the provided attributes.

The architectural arrangement for this dataset involves the utilization of 15 ensemble reservoirs. This choice of model configuration is underpinned by the aim to effectively capture the intricacies inherent in the absenteeism data and its relationship to social drinking behavior. Employing ensemble reservoirs empowers the model to discern nuanced patterns and interactions among the attributes, thereby enhancing its classification accuracy.

• Temperature Readings: IOT Devices: ⁶ The dataset pertaining to temperature readings from IoT devices centers on the recordings captured by these devices, both inside and outside an undisclosed room (referred to as the admin room). This dataset comprises temperature readings and is characterized by five distinct features. In total, the dataset encompasses 97605 samples.

The primary objective in this analysis involves binary classification, where the aim is to classify temperature readings based on whether they originate from an IoT device installed inside the room or outside it. The target column holds the binary class labels indicating the origin of the temperature reading.

In terms of dataset characteristics, the architecture of our model involves the utilization of 15 ensemble reservoirs. This architectural choice is rooted in the desire to effectively capture the underlying patterns and distinctions present within the temperature readings dataset. The use of ensemble reservoirs enhances the model's capacity to distinguish between the different temperature reading sources, thereby facilitating accurate classification.

B Algorithm for RT

In the pseudo algorithm 1, we describe how to train RT models. The algorithm initiates by setting parameters for both the Transformer and the reservoir groups. During each training epoch, it processes sequences incrementally from a specified start time k up to the total length T. Each sequence segment transforms an embedded vector, which is then input into the reservoirs to produce intermediate representations. These are subsequently merged with the original embedded input, controlled by a weighting parameter κ , forming a composite feature vector. This vector is fed into the Transformer to predict future sequence values. The training cycle completes by calculating loss between the predicted and actual values and updating the model parameters accordingly, aiming to minimize prediction errors in following epochs.

C Variable Descriptions

We have described the used variables and math notations in Table 9.

D Baselines

We show our experimental results of Reservoir Transformer (RT) compared to baselines, including state-of-the-art methods in time-series prediction, such as FEDformer [Zhou et al., 2022], Autoformer [Wu et al., 2021], Informer [Zhou et al., 2021], Pyraformer [Liu et al., 2021], log(T)rans [Li et al., 2019], GRIN [Cini et al., 2021], BRITS [Cao et al., 2018], STMVL [Yi et al., 2016], M-RNN [Yoon et al., 2018], ImputeTS [Moritz and Bartz-Beielstein, 2017], and Transformer Vaswani et al. [2017]. To conduct experiments on multivariate and uni-variate time series, we evaluate methods outlined by [Zeng et al., 2022], which includes data splitting, pre-processing, and parameter setting.

E Long Uni-Variate Forecasting

In Table 10 we have compared the long uni-variate time-series forecasting with state of the art time series method and showed improvement of RT in uni-variate forecasting.

F More results

Table 11 shows that RT model outperforms GRIN [Cini et al., 2021], BRITS [Cao et al., 2018], ST-MVL [Yi et al., 2016], M-RNN [Yoon et al., 2018], ImputeTS [Moritz and Bartz-Beielstein, 2017] on the air quality dataset. On regression and classification tasks, RT consistently outperforms the baseline Transformer with respect to all criteria, achieving significantly lower MSE and MAE values across various datasets like DWV, DGP, DDFO, and BTC. This suggests that the RT model is better equipped to capture complex temporal patterns. In the classification tasks, the RT model demonstrates better performance in terms of accuracy, F1 Score, Jaccard Score, Roc Auc, Precision, and Recall across different datasets like Absenteeism at work and Temperature Readings. Through this analysis, we provide evidence that the RT architecture excels not only in regression tasks but also in classification tasks, outperforming traditional Transformer architectures. Additionally, we have shown the comparison of multi-variate time series with other methods such as LightTS [Campos et al., 2023] and Autformer [Wu et al., 2021] in Table 11.

G More Ablation Analysis

G.1 Look-Back Window Size vs Loss

In Figure 5, we have proved that RT works for the short look-back window better than the Dlinear method, since RT can capture the long-term dependencies using group reservoirs.

⁴https://finance.yahoo.com/quote/BTC-USD/history/

⁵https://archive.ics.uci.edu/ml/datasets/Absenteeism+at+work

⁶https://www.kaggle.com/datasets/atulanandjha/temperature-readings-iot-devices

Variable	Description
M(.)	Transformer model
$\mathcal{R}(.)$	Deep reservoir computing
$\overline{\mathbf{u}_t}$	Input at t time steps
\mathbf{x}_t	Reservoir state at t time steps
\mathbf{y}_t	Linear output of reservoir
$\mathbf{\hat{h}}_{t}$	Embedding of time steps
$oldsymbol{\Lambda}_t$	Non-linear readout
\mathbf{z}_t	Self attention of group reservoir
\mathbf{o}_t	Ensembling of group reservoir
\mathbf{f}_t	Input of Transformer
\overline{T}	Total time input length
k	Look back window
H	Number of attention heads
N_r	Reservoir size
N_u	Reservoir input size
m	Reservoir output size
L	Number of reservoirs in Group
h	Forecasting horizons
d_{ϵ}	Model dimension
d_{key}	Dimension of key in attention
d_{value}	Dimension of key in attention
l_y	Number of layers in Transformer
c	Compressive Transformer memory size
r	Compression ratio
p	Number of soft-prompt summary vectors
s	Kernel size
P	Patch size
Φ	Transformer's learnable parameters
\mathbf{W}_q	Queries weights
\mathbf{W}_v	Values weights
\mathbf{W}_k	Keys weights
\mathbf{W}_{in}	Input-to-reservoir weight matrix
\mathbf{W}	Reservoir weight matrix
heta	Bias-to-reservoir weight
\mathbf{W}_{out}	Reservoir-to-readout weight matrix
$oldsymbol{ heta}_{out}$	Bias-to-readout weight

Table 9: Descriptions of all variables used in this paper

Metho	ods	F	T	Lin	ear	NLi	near	DLi	near	FEDF	rmer-f	FEDFo	rmer-w	Autof	ormer	Info	rmer	log(T)rans
Metri	ic	MSE	MAE	MSE	MAE	MSE	MAE	MSE	MAE	MSE	MAE								
	96	0.050	0.172	0.189	0.359	0.053	0.177	0.056	0.180	0.079	0.215	0.080	0.214	0.071	0.206	0.193	0.377	0.283	0.468
	192	0.064	0.201	0.078	0.212	0.069	0.204	0.071	0.204	0.104	0.245	0.105	0.256	0.114	0.262	0.217	0.395	0.234	0.409
ETTh1	336	0.081	0.225	0.091	0.237	0.081	0.226	0.098	0.244	0.119	0.270	0.120	0.269	0.107	0.258	0.202	0.381	0.386	0.546
	720	0.097	0.292	0.172	0.340	0.080	0.226	0.189	0.359	0.142	0.299	0.127	0.280	0.126	0.283	0.183	0.355	0.475	0.629
	96	0.127	0.275	0.133	0.283	0.129	0.278	0.131	0.279	0.128	0.271	0.156	0.306	0.153	0.306	0.213	0.373	0.217	0.379
	192	0.168	0.324	0.176	0.330	0.169	0.324	0.176	0.329	0.185	0.330	0.238	0.380	0.204	0.351	0.227	0.387	0.281	0.429
ETTh2	336	0.192	0.351	0.213	0.371	0.194	0.355	0.209	0.367	0.231	0.378	0.271	0.412	0.246	0.389	0.242	0.401	0.293	0.437
	720	0.369	0.411	0.292	0.440	0.225	0.381	0.276	0.426	0.278	0.420	0.288	0.438	0.268	0.409	0.291	0.439	0.218	0.387
	96	0.024	0.119	0.028	0.125	0.026	0.122	0.028	0.123	0.033	0.140	0.036	0.149	0.056	0.183	0.109	0.277	0.049	0.171
	192	0.037	0.149	0.043	0.154	0.039	0.149	0.045	0.156	0.058	0.186	0.069	0.206	0.081	0.216	0.151	0.310	0.157	0.317
ETTm1	336	0.050	0.168	0.059	0.180	0.052	0.172	0.061	0.182	0.084	0.231	0.071	0.209	0.076	0.218	0.427	0.591	0.289	0.459
	720	0.072	0.199	0.080	0.211	0.073	0.207	0.080	0.210	0.102	0.250	0.105	0.248	0.110	0.267	0.438	0.586	0.430	0.579
-	96	0.062	0.182	0.066	0.189	0.063	0.182	0.063	0.183	0.067	0.198	0.063	0.189	0.065	0.189	0.088	0.225	0.075	0.208
	192	0.092	0.224	0.094	0.230	0.090	0.223	0.092	0.227	0.102	0.245	0.110	0.252	0.118	0.256	0.132	0.283	0.129	0.275
ETTm2	336	0.115	0.258	0.120	0.263	0.117	0.259	0.119	0.261	0.130	0.279	0.147	0.301	0.154	0.305	0.180	0.336	0.154	0.302
	720	0.356	0.382	0.175	0.320	0.170	0.318	0.175	0.115	0.178	0.325	0.219	0.368	0.182	0.335	0.300	0.435	0.160	0.321

Table 10: Univariate long-term forecasting results

G.2 Graphical Explanation of Features

In Figure 6, we present a visual depiction that offers a comprehensive insight into the interpretability of features derived from both the reservoir output \mathbf{z}_t and input feature \mathbf{u}_t .

			Air Qu	ality				
Metric/Model	GRIN	BRITS	ST-MVL	M-RNN	ImputeTS	RT		
MAE	10.514	12.242	12.124	14.242	19.584	9.046		
Method		Training			Test			
REGRESSION	TASKS							
Model/Metric	MSE	MAE	R2	MSE	MAE	R2	Parameters	
			Daily website v	isitors (DWV)				
Baseline	98.45	7.583	0.996	42.95	5.181	0.997	∼13.2k	
RT	10.400 (-89.43%)	2.114	0.999	6.181	1.893	0.999	\sim 3.2k	
			Daily Gold P	rice (DGP)				
Baseline	39459.790	112.251	0.996	168608.260	353.310	0.959	∼13.9k	
RT	22022.981	86.985	0.998	28790.317	119.227	0.994	\sim 3.4k	
		Dai	ly Demand Forecas	sting Orders (DD	FO)			
Baseline	312.933	13.274	0.929	1013.962	22.265	0.099	∼14.1k	
RT	76.385	7.487	0.985	410.652	10.173	0.720	\sim 3.7k	
			Bitcoin Historical	Dataset (BTC)				
Baseline	188614.931	427.801	0.968	79389.491	232.119	0.961	∼10.5k	
RT	158651.081	310.918	0.998	74800.535	211.626	0.989	\sim 2.8k	
CLASSIFICAT	TON TASKS:							
Model	Accuracy	F1 Score	Jaccard Score	Roc Auc	Precision	Recall	Parameters	
			Absenteeisi	n at work				
Baseline	0.928	0.940	0.887	0.929	0.953	0.927	∼14.2k	Trainin
RT	0.947	0.956	0.916	0.950	0.976	0.936	\sim 3.5k	Trainin
Baseline	0.844	0.839	0.722	0.844	0.833	0.845	∼14.2k	Test
RT	0.899	0.901	0.819	0.901	0.944	0.860	\sim 3.5k	Test
			Temperature	Readings				
Baseline	0.888	0.934	0.877	0.877	0.877	0.915	∼10.9k	Trainin
RT	0.959	0.975	0.952	0.934	0.981	0.970	\sim 2.3k	Trainin
Baseline	0.649	0.688	0.524	0.646	0.632	0.755	∼10.9k	Test
RT	0.802	0.843	0.728	0.794	0.867	0.820	\sim 2.3k	Test

Table 11: Assessing the performance of regression on both training and test datasets, we utilize a window size of 100 to observe historical data in baseline Transformers and RT.

G.3 Non-Linear output

In Table 13, we present a comparison of the non-linear readout of the reservoir using different activation functions.

H Limitations

Our method assumes that the compressed memory represents the long context within the time-series data. However, in practice memory compression can result in potential information loss. Therefore, giving the whole context as input instead of compressing it to a fixed size may result in better performance. Additionally, we evaluated our method on standard time-series benchmarks and thus set the maximum horizon value as 720. There may exist datasets that have extremely long-term dependencies. To capture this dependency in such datasets, we would either have to increase the size of the reservoir's input.

Method	ls		T urs)		near (23)		hTST 023)	Time (20	esNet		ormer (22)	Statio	onary	ETSfe (20		Ligl (20		Autof	
Metric		MSE	MAE	MSE	MAE	MSE	MAE	MSE	MAE	MSE	MAE	MSE	MAE	MSE	MAE	MSE	MAE	MSE	MAE
Metric	96	0.362	0.392	0.376	0.397	0.375	0.399	0.370	0.399	0.384	0.402	0.376	0.419	0.449	0.479	0.424	0.432	0.449	0.459
	192	0.396	0.412	0.405	0.416	0.413	0.421	0.436	0.429	0.420	0.448	0.534	0.504	0.538	0.504	0.475	0.462	0.500	0.482
ETTh1	336	0.427	0.422	0.439	0.443	0.422	0.436	0.491	0.469	0.459	0.465	0.588	0.535	0.574	0.521	0.518	0.488	0.521	0.496
	720	0.441	0.455	0.472	0.490	0.447	0.466	0.521	0.500	0.506	0.507	0.643	0.616	0.562	0.535	0.547	0.533	0.514	0.512
	avg	0.406	0.418	0.422	0.437	0.413	0.430	0.458	0.450	0.440	0.460	0.570	0.537	0.542	0.510	0.491	0.479	0.496	0.487
	96	0.262	0.320	0.289	0.353	0.274	0.336	0.340	0.374	0.358	0.397	0.476	0.458	0.340	0.391	0.397	0.437	0.346	0.388
	192	0.331	0.373	0.383	0.418	0.339	0.379	0.402	0.414	0.429	0.439	0.512	0.493	0.430	0.439	0.520	0.504	0.456	0.452
ETTh2	336	0.358	0.403	0.448	0.465	0.329	0.380	0.452	0.452	0.496	0.487	0.552	0.551	0.485	0.479	0.626	0.559	0.482	0.486
	720	0.369	0.411	0.605	0.551	0.379	0.422	0.462	0.468	0.463	0.474	0.562	0.560	0.500	0.497	0.863	0.672	0.515	0.511
	avg	0.330	0.376	0.431	0.446	0.330	0.379	0.414	0.427	0.437	0.449	0.526	0.516	0.439	0.452	0.602	0.543	0.450	0.459
-	96	0.272	0.336	0.299	0.343	0.290	0.342	0.338	0.375	0.379	0.419	0.386	0.398	0.375	0.398	0.374	0.400	0.505	0.475
	192	0.310	0.357	0.335	0.365	0.332	0.369	0.374	0.387	0.426	0.441	0.459	0.444	0.408	0.410	0.400	0.407	0.553	0.496
ETTm1	336	0.351	0.382	0.369	0.386	0.366	0.392	0.410	0.411	0.445	0.459	0.495	0.464	0.435	0.428	0.438	0.438	0.621	0.537
	720	0.380	0.409	0.425	0.421	0.416	0.420	0.478	0.450	0.543	0.490	0.585	0.516	0.499	0.462	0.527	0.502	0.671	0.561
	avg	0.328	0.371	0.357	0.378	0.351	0.380	0.400	0.406	0.448	0.452	0.481	0.456	0.429	0.425	0.435	0.437	0.588	0.517
	96	0.163	0.254	0.167	0.269	0.165	0.255	0.187	0.267	0.203	0.287	0.192	0.274	0.189	0.280	0.209	0.308	0.255	0.339
	192	0.218	0.290	0.224	0.303	0.220	0.292	0.249	0.309	0.269	0.328	0.280	0.339	0.253	0.319	0.311	0.382	0.281	0.340
ETTm2	336	0.271	0.328	0.281	0.342	0.274	0.329	0.321	0.351	0.325	0.366	0.334	0.361	0.314	0.357	0.442	0.466	0.339	0.372
	720	0.356	0.382	0.397	0.421	0.362	0.385	0.408	0.403	0.421	0.415	0.417	0.413	0.414	0.413	0.675	0.587	0.433	0.432
	avg	0.252	0.316	0.267	0.333	0.255	0.315	0.291	0.333	0.305	0.349	0.371	0.306	0.347	0.293	0.342	0.409	0.436	0.327
	96	0.146	0.196	0.176	0.237	0.149	0.198	0.172	0.220	0.217	0.296	0.173	0.223	0.197	0.281	0.182	0.242	0.266	0.336
	192	0.193	0.236	0.220	0.282	0.194	0.241	0.219	0.261	0.276	0.336	0.245	0.285	0.237	0.312	0.227	0.287	0.307	0.367
Weather	336	0.239	0.240	0.265	0.319	0.245	0.282	0.280	0.306	0.339	0.380	0.321	0.338	0.298	0.353	0.282	0.334	0.359	0.395
	720	0.301	0.316	0.333	0.362	0.314	0.334	0.365	0.359	0.403	0.428	0.414	0.410	0.352	0.288	0.352	0.386	0.419	0.428
	avg	0.219	0.247	0.248	0.300	0.225	0.264	0.259	0.287	0.309	0.360	0.288	0.314	0.271	0.334	0.261	0.312	0.338	0.382
	96 192	0.130	0.219 0.243	0.140 0.153	0.237 0.249	0.129 0.157	0.222 0.240	0.168	0.272 0.289	0.193	0.308	0.169 0.182	0.273 0.286	0.187 0.199	0.304 0.315	0.207	0.307 0.316	0.201 0.222	0.317 0.334
Electricity		0.154	0.245		0.249	0.157	0.240	0.184	0.289	0.201	0.313	0.182	0.286	0.199	0.313	0.213	0.316	0.222	0.334
Electricity	336 720	0.158	0.245	0.169	0.267	0.163	0.259	0.198	0.300	0.214	0.329	0.200	0.304	0.212	0.345	0.230	0.333	0.231	0.338
	avg	0.150	0.251	0.203	0.361	0.197	0.252	0.192	0.320	0.246	0.333	0.193	0.321	0.233	0.343	0.203	0.300	0.234	0.338
	96	0.138	0.231	0.100	0.282	0.360	0.232	0.192	0.321	0.587	0.366	0.612	0.238	0.607	0.323	0.615	0.329	0.613	0.388
	192	0.376	0.250	0.423	0.282	0.379	0.256	0.617	0.321	0.604	0.373	0.613	0.340	0.621	0.392	0.601	0.382	0.616	0.382
Traffic	336	0.370	0.268	0.436	0.296	0.379	0.264	0.629	0.336	0.621	0.373	0.618	0.340	0.622	0.396	0.613	0.386	0.622	0.337
Traine	720	0.426	0.382	0.466	0.315	0.432	0.286	0.640	0.350	0.626	0.382	0.653	0.355	0.632	0.396	0.658	0.407	0.660	0.408
	avg	0.386	0.261	0.433	0.295	0.390	0.263	0.620	0.336	0.610	0.376	0.628	0.379	0.624	0.340	0.621	0.396	0.622	0.392
-	24	1.301	0.739	2.215	1.081	1.319	0.754	2.317	0.934	3.228	1.260	2.294	0.945	2.527	1.020	8.313	2.144	3.483	1.287
	36	1.409	0.824	1.963	0.963	1.430	0.834	1.972	0.920	2.679	1.080	1.825	0.848	2.615	1.007	6.631	1.902	3.103	1.148
ILI	48	1.520	0.807	2.130	1.024	1.553	0.815	2.238	0.940	2.622	1.078	2.010	0.900	2.359	0.972	7.299	1.982	2.669	1.085
	60	1.553	0.852	2.368	1.096	1.520	0.788	2.027	0.928	2.857	1.157	2.178	0.963	2.487	1.016	7.283	1.985	2.770	1.125
	avg	1.439	0.805	2.169	1.041	1.443	0.797	2.139	0.931	2.847	1.144	2.077	0.914	2.497	1.004	7.382	2.003	3.006	1.161

Table 12: Multivariate long-term time-series forecasting: lower values indicate better performance. Forecasting horizons are $h \in \{24, 36, 48, 60\}$ for ILI and $h \in \{96, 192, 336, 720\}$ for the rest.

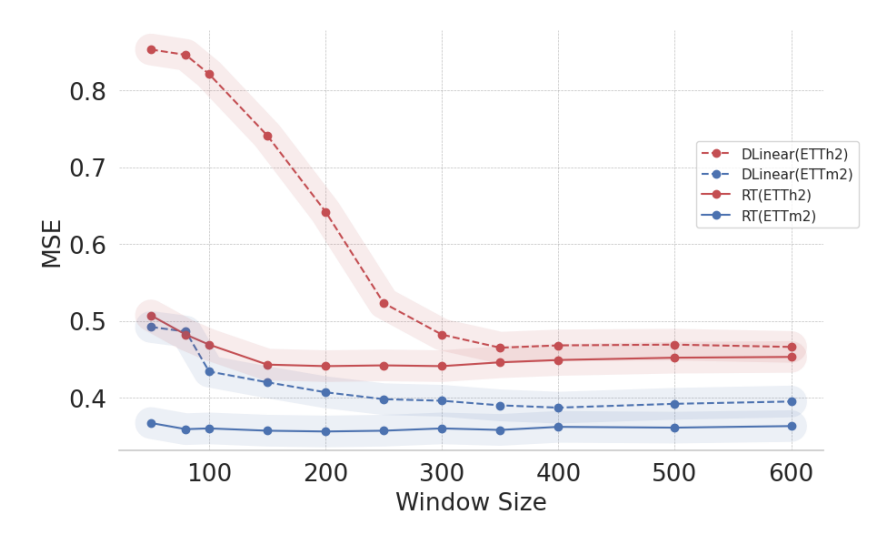


Figure 5: Look back window size vs loss

Activation			ETTh1				ETTh2				Traffic	
Activation	Linear	ReLu	Tanh	Self-Attention	Linear	ReLu	Tanh	Self-Attention	Linear	ReLu	Tanh	Self-Attention
MSE	0.538	0.462	0.474	0.441	0.447	0.608	0.495	0.485	0.498	0.428	0.463	0.426
MAE	0.562	0.470	0.475	0.455	0.348	0.552	0.468	0.478	0.327	0.293	0.314	0.281

Table 13: Comparison of MSE for different readout activation.

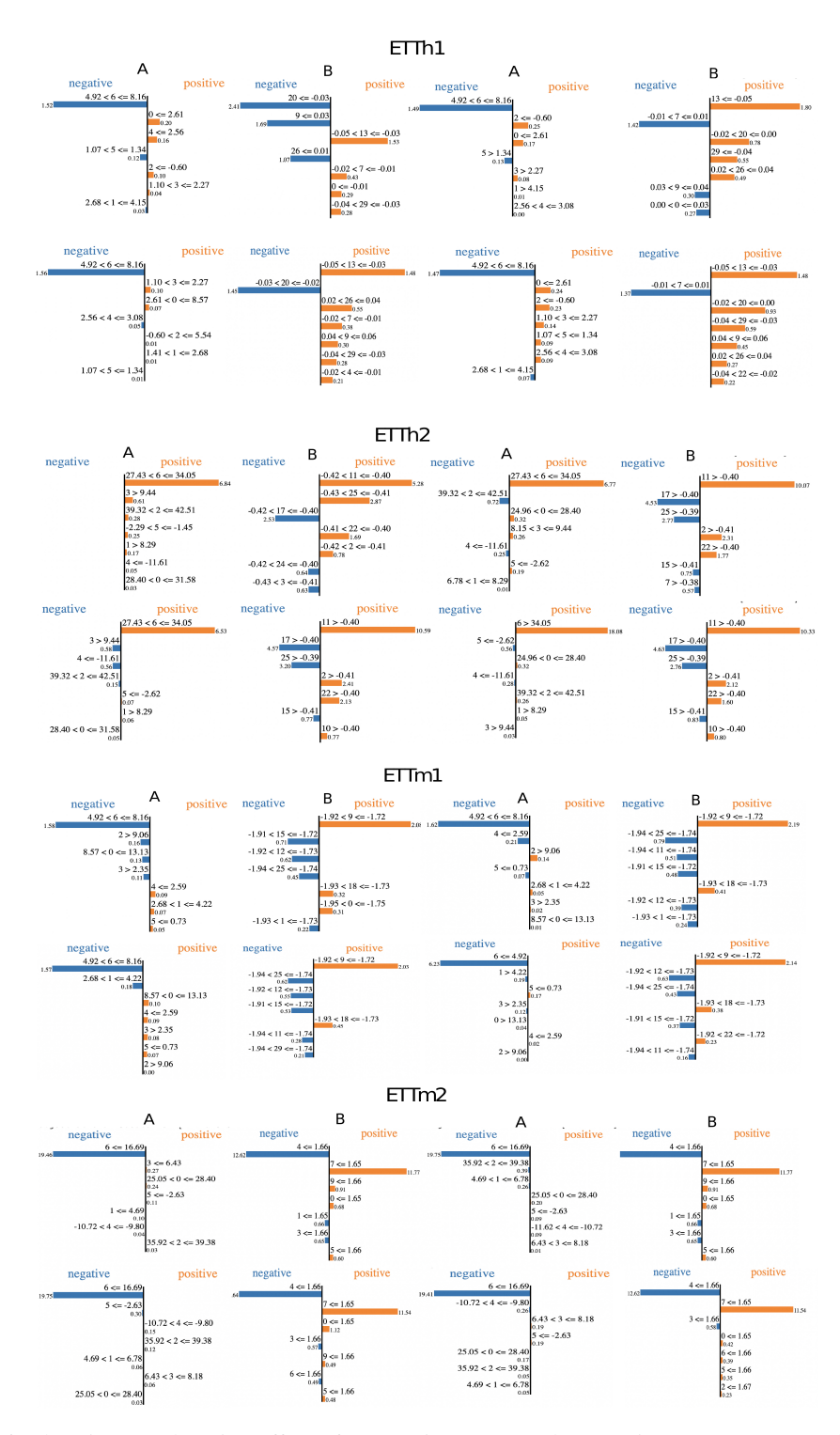


Figure 6: The Lime Explanation effect of current input (A) and reservoir (B) on output prediction is shown. The test dataset is represented by ETTh1, ETTh2, ETTm1, and ETTm2. The results indicate that current input has a greater impact on feature 6, while the reservoir affects multiple features such as 20, 13, 29, and 7.